

Article

CCSD(T) Rotational Constants for Highly Challenging C₅H₂ Isomers—A Comparison between Theory and Experiment

Venkatesan S. Thimmakonda ^{1,*}  and Amir Karton ^{2,*} 

¹ Department of Chemistry and Biochemistry, San Diego State University, San Diego, CA 92182-1030, USA

² School of Science and Technology, University of New England, Armidale, NSW 2351, Australia

* Correspondence: vthimmakondusamy@sdsu.edu (V.S.T.); amir.karton@une.edu.au (A.K.)

Abstract: We evaluate the accuracy of CCSD(T) and density functional theory (DFT) methods for the calculation of equilibrium rotational constants (A_e , B_e , and C_e) for four experimentally detected low-lying C₅H₂ isomers (ethynylcyclopropenylidene (**2**), pentatetraenylidene (**3**), ethynylpropadienylidene (**5**), and 2-cyclopropen-1-ylidenethenylidene (**8**)). The calculated rotational constants are compared to semi-experimental rotational constants obtained by converting the vibrationally averaged experimental rotational constants (A_0 , B_0 , and C_0) to equilibrium values by subtracting the vibrational contributions (calculated at the B3LYP/jun-cc-pVTZ level of the theory). The considered isomers are closed-shell carbenes, with cumulene, acetylene, or strained cyclopropene moieties, and are therefore highly challenging from an electronic structure point of view. We consider both frozen-core and all-electron CCSD(T) calculations, as well as a range of DFT methods. We find that calculating the equilibrium rotational constants of these C₅H₂ isomers is a difficult task, even at the CCSD(T) level. For example, at the all-electron CCSD(T)/cc-pwCVTZ level of the theory, we obtain percentage errors $\leq 0.4\%$ (C_e of isomer **3**, B_e and C_e of isomer **5**, and B_e of isomer **8**) and 0.9–1.5% (B_e and C_e of isomer **2**, A_e of isomer **5**, and C_e of isomer **8**), whereas for the A_e rotational constant of isomers **2** and **8** and B_e rotational constant of isomer **3**, high percentage errors above 3% are obtained. These results highlight the challenges associated with calculating accurate rotational constants for isomers with highly challenging electronic structures, which is further complicated by the need to convert vibrationally averaged experimental rotational constants to equilibrium values. We use our best CCSD(T) rotational constants (namely, ae-CCSD(T)/cc-pwCVTZ for isomers **2** and **5**, and ae-CCSD(T)/cc-pCVQZ for isomers **3** and **8**) to evaluate the performance of DFT methods across the rungs of Jacob's Ladder. We find that the considered pure functionals (BLYP-D3BJ, PBE-D3BJ, and TPSS-D3BJ) perform significantly better than the global and range-separated hybrid functionals. The double-hybrid DSD-PBEP86-D3BJ method shows the best overall performance, with percentage errors below 0.5% in nearly all cases.

Keywords: C₅H₂; interstellar medium; astrochemistry; rotational constants; CCSD(T); DFT



Citation: Thimmakonda, V.S.; Karton, A. CCSD(T) Rotational Constants for Highly Challenging C₅H₂ Isomers—A Comparison between Theory and Experiment. *Molecules* **2023**, *28*, 6537. <https://doi.org/10.3390/molecules28186537>

Academic Editor: Cristina Puzzarini and Silvia Alessandrini

Received: 30 July 2023

Revised: 6 September 2023

Accepted: 7 September 2023

Published: 9 September 2023



Copyright: © 2023 by the authors. Licensee MDPI, Basel, Switzerland. This article is an open access article distributed under the terms and conditions of the Creative Commons Attribution (CC BY) license (<https://creativecommons.org/licenses/by/4.0/>).

1. Introduction

Rotational spectroscopy is one of the most powerful spectroscopic tools for accurately identifying the structural information of molecules in the gas phase [1,2]. Prediction of accurate rotational constants using quantum chemical methods facilitates the laboratory analysis of rotational spectroscopists by carrying out the laboratory search in a relatively narrow range and consequently identifying the detection of unknown molecules [3–13]. However, in order to predict the rotational constants with sufficient accuracy, high levels of the theory, which can be computationally quite demanding, have to be employed [14–16]. To be precise, the percent error between the theory and an experiment should not be larger than 0.2% [17,18]. Recent theoretical studies by Puzzarini and Stanton advocate for 0.1% accuracy in order to be useful to rotational spectroscopists, in particular for small- to medium-sized molecules (that is, up to 20 atoms) [19]. These very small percent errors are

required, since larger percent errors lead to a wider range in the laboratory search, which is not only cumbersome, but may also lead to inconclusive outcomes.

Until now, five C_5H_2 isomers, namely, linear pentadiynylidene (**1**) [20–26], ethynylcyclopropenylidene (**2**) [6,23,26], pentatetraenylidene (**3**) [2,21,24], ethynylpropadienylidene (**5**) [21,27], and 2-cyclopropen-1-ylidenethenylidene (**8**) [25,27] have been identified in the laboratory (see Figure 1). Using Fourier Transform Microwave (FTMW) spectroscopy, McCarthy and co-workers had identified four closed-shell carbene isomers of C_5H_2 (**2**, **3**, **5** and **8**), whose dipole moments are non-zero ($\mu \neq 0$). Due to symmetry ($D_{\infty h}$), isomer **1** lacks a permanent dipole and, therefore, this molecule is unsuitable for rotational spectroscopic observations and radioastronomical studies. Among the four polar carbenes that were identified in the laboratory, the cumulene carbene isomer (**3**) was reported initially [2]. Later, the laboratory detection of the three-membered ring-chain isomer (**2**) was also reported with both *a*- and *b*-type rotational transitions, as the inertial axis dipole moment components are in two directions for this molecule [6]. Both of these molecules (**3** and **2**) are higher homologues of propadienylidene (a cumulene carbene isomer of C_3H_2) and cyclopropenylidene, respectively. In addition, the latter are known to exist in the interstellar medium (ISM) [28,29]. The laboratory detection of C_3H_2 isomers was undoubtedly very helpful in the identification of the same in the ISM [28,30]. Three isotopologues of C_3H_2 , the doubly deuterated $c\text{-}C_3D_2$, singly deuterated $c\text{-}C_3HD$, and one species of $c\text{-}H^{13}CC_2H$ (^{13}C off of the principal axis of the molecule) have been detected in two starless cores [31–34]. In 2021, two of the polar C_5H_2 isomers, **2** and **3**, were identified in the Taurus Molecular Cloud-1 (TMC-1) [35,36]. Though numerous theoretical studies have been carried out in the past, the focus was mostly on the structure, energetics, and spectroscopic properties of the low-lying isomers alone that were observed in the laboratory [3,9,20–25,37–44]. A comprehensive study related to the accuracy of rotational constants with various theoretical methods has not been carried out so far and, thus, the objective of the present article focuses on that front.

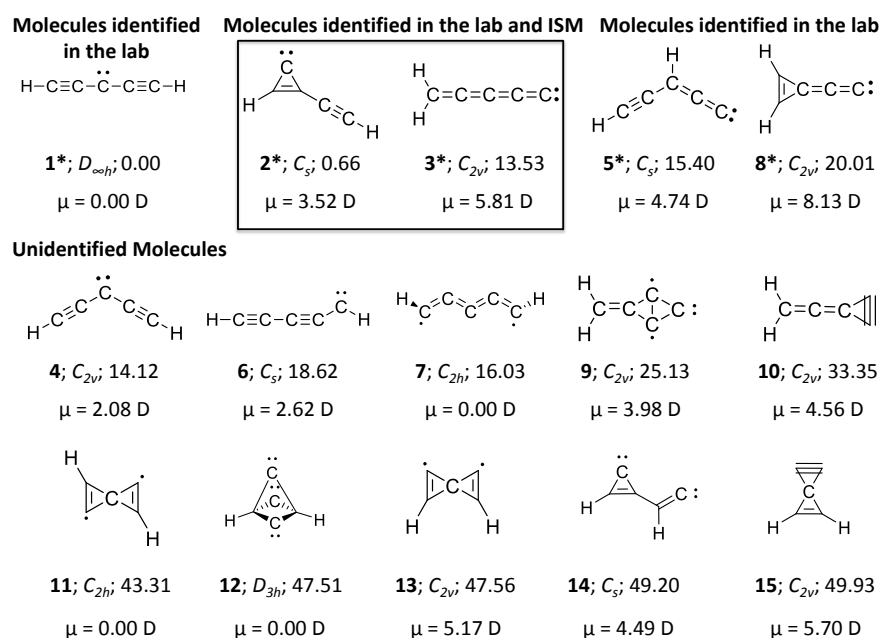


Figure 1. C_5H_2 isomers considered in this work. ZPVE-corrected relative energies are calculated at the CCSDT(Q)/CBS level of the theory (in kcal mol^{-1}). Dipole moments (in Debye) and ZPVEs are computed at the CCSD(T)/cc-pVTZ level of the theory. Experimentally detected isomers are marked with an asterisk. Isomer **1** is a triplet and all others are singlets. Note that isomers **10** and **15** are transition states, isomer **7** is a second-order saddle-point, and all others are local minima.

It should be noted that the electronic structure of the C_5H_2 isomers in Figure 1 renders these isomers challenging from the electronic structure point of view. As illustrated in Figure 1, these isomers are characterized by carbenes (mono, bi, or tri), biradicals, polyynics, molecules with a planar tetracoordinate carbon (ptC) atom [15,43,45–49] or cumulenic electronic structures [41–43]. In addition, several isomers are associated with high strain energies. Therefore, these isomers are expected to be challenging for density functional theory (DFT) methods, and high-level ab initio methods such as coupled-cluster with single, double, and quasiperturbative triple excitations (CCSD(T)) [50–53] are needed for an adequate description of the electronic structure of these isomers. Having said that, the CCSD(T) method at the complete basis set (CBS) limit has been found to reproduce the relative energies of the C_5H_2 isomers with sub-chemical accuracy (i.e., with deviations from CCSDT(Q)/CBS energies below 1 kcal mol^{-1}) [41–43,54].

2. Computational Details

Geometry optimizations and frequency calculations for all C_5H_2 isomers are carried out with 12 different density functionals with the cc-pVQZ basis set [55]. The considered DFT functionals are: PBE [56], BLYP [57,58], M06-L [59,60], TPSS [61,62], B3LYP [57,58,63,64], PBE0 [65], BMK [66], M06-2X [60], ω B97X-D [67], CAM-B3LYP [68], B2-PLYP [69], and DSD-PBEP86 [70]. To account for London dispersion interactions [71], Grimme's empirical dispersion corrections (D3) [72] with Becke-Johnson damping (D3BJ) [73,74] has been included in all DFT calculations except M06-L, M06-2X, and ω B97X-D, where dispersion effects are already accounted for. All DFT calculations are carried out with the Gaussian 16 program suite [75]. Apart from using DFT, both geometry optimization and frequency calculations were also performed using coupled-cluster (CC) methods with singles and doubles (CCSD) [76,77] augmented with perturbative treatments of triple excitations (CCSD(T)) to incorporate a high-level treatment of electron correlation effects [50–52]. We have used Dunning's correlation consistent polarized valence double, triple, and quadruple zeta (cc-pVnZ; $n = D, T, \text{ and } Q$) basis sets [55] in these calculations. The frozen-core (fc) approximation is utilized (i.e., the carbon 1s orbitals are frozen) in these calculations. All-electron (ae) CCSD(T) calculations were also carried out, and we have used both core-valence (cc-pCVnZ; $n = T, \text{ and } Q$) [78] and weighted core-valence (cc-pwCVTZ) [79] basis sets in these cases. We note that the fc-CCSD(T)/cc-pVTZ level of the theory has been found to give accurate equilibrium geometries with a mean absolute deviation of only 0.003 \AA relative to CCSD(T)/CBS bond distances for a wide and diverse set of the 122 species with up to five non-hydrogen atoms [80]. Harmonic vibrational frequencies were computed at the same levels of the theory by analytic calculation of second derivatives for all stationary points [81]. All CCSD(T) calculations were carried out with the CFOUR program package [82]. For the sake of simplicity, hereinafter, CCSD(T) will be denoted by CC.

3. Results and Discussion

Let us begin with the CC results for the molecules that have been synthesized in the laboratory (isomers 2, 3, 5, and 8 shown in Figure 1). Table 1 lists the equilibrium CC rotational constants along with the semi-experimental rotational constants for isomer 2, 3, 5, and 8. We begin by noting that the deviations between the theory and experiments are very large for the A_e rotational constant for the isomers 2 and 8, both of which contain a highly strained cyclopropene ring. It should be noted, however, that excluding these three problematic rotational constants, the percentage errors obtained for the other isomers at the fc-CC/cc-pVTZ level of the theory are on par with those obtained at the same level of the theory for a set of less challenging small molecules in reference [17]. For the three problematic rotational constants (A_e for isomers 2 and 8 and B_e for isomer 3), we obtain very high percentage errors of 6.3–10.4% across the various CC levels of the theory in Table 1. These high percentage errors indicate that the A_e rotational constant for these isomers poses a challenge even at the CC level. However, these large deviations between the theory and our semi-experimental values may also be attributed to the B3LYP/jun-cc-pVTZ vibrational

corrections used to convert the experimental A_0 rotational constant to semi-experimental equilibrium A_e values that can be compared with the CC equilibrium values. Obtaining the vibrational corrections at higher levels of the theory (e.g., at the CC level) proved beyond our available computational resources.

Table 1. Theoretical equilibrium rotational constants (A_e , B_e , C_e ; in MHz) obtained at the CCSD(T) level using different basis sets (with and without the frozen-core approximation) along with semi-experimental rotational constants for isomers **2**, **3**, **5**, and **8** of C_5H_2 ^a.

| Isomer | Level of the Theory ^b | Rotational Constants | | | % Error | | |
|----------|----------------------------------|-------------------------|---------|---------|---------------------|-------|-------|
| | | A_e | B_e | C_e | A_e | B_e | C_e |
| 2 | Semi-Experimental ^c | 36,972.92 | 3448.64 | 3154.31 | - | - | - |
| | fc-CC/VDZ | 33,109.37 | 3309.59 | 3008.83 | -10.45 [§] | -4.03 | -4.61 |
| | fc-CC/VTZ | 34,266.70 | 3394.14 | 3088.25 | -7.32 [§] | -1.58 | -2.09 |
| | fc-CC/VQZ | 34,547.62 | 3409.12 | 3102.93 | -6.56 [§] | -1.15 | -1.63 |
| | ae-CC/VDZ | 33,184.61 | 3315.35 | 3014.21 | -10.25 [§] | -3.87 | -4.44 |
| | ae-CC/VTZ | 34,640.92 | 3429.06 | 3120.20 | -6.31 [§] | -0.57 | -1.08 |
| | ae-CC/CVTZ | 34,465.55 | 3408.64 | 3101.86 | -6.78 [§] | -1.16 | -1.66 |
| | ae-CC/CVTZ | 34,544.69 | 3414.01 | 3106.95 | -6.57 [§] | -1.00 | -1.50 |
| 3 | Semi-Experimental ^d | 231,551.05 ^e | 2216.88 | 2283.64 | - | - | - |
| | fc-CC/VDZ | 282,533.83 | 2219.13 | 2201.84 | N/A | 0.10 | -3.58 |
| | fc-CC/VTZ | 289,957.56 | 2280.08 | 2262.29 | N/A | 2.85 | -0.93 |
| | fc-CC/VQZ | 290,263.96 | 2289.74 | 2271.82 | N/A | 3.29 | -0.52 |
| | ae-CC/VDZ | 283,066.03 | 2223.09 | 2205.77 | N/A | 0.28 | -3.41 |
| | ae-CC/VTZ | 292,400.34 | 2302.87 | 2284.87 | N/A | 3.88 | 0.05 |
| | ae-CC/CVTZ | 290,592.49 | 2289.69 | 2271.79 | N/A | 3.28 | -0.52 |
| | ae-CC/wCVTZ | 290,836.71 | 2293.17 | 2275.23 | N/A | 3.44 | -0.37 |
| | ae-CC/CVQZ | 291,115.51 | 2300.31 | 2282.27 | N/A | 3.76 | -0.06 |
| 5 | Semi-Experimental ^f | 31,151.23 | 2863.13 | 2621.54 | - | - | - |
| | fc-CC/VDZ | 30,282.06 | 2769.12 | 2537.12 | -2.79 | -3.28 | -3.22 |
| | fc-CC/VTZ | 31,364.94 | 2832.59 | 2597.97 | 0.69 | -1.07 | -0.90 |
| | fc-CC/VQZ | 31,248.01 | 2850.63 | 2612.32 | 0.31 | -0.44 | -0.35 |
| | ae-CC/VDZ | 30,321.18 | 2774.08 | 2541.55 | -2.66 | -3.11 | -3.05 |
| | ae-CC/VTZ | 32,467.69 | 2842.48 | 2613.66 | 4.23 | -0.72 | -0.30 |
| | ae-CC/CVTZ | 31,402.16 | 2846.75 | 2610.13 | 0.81 | -0.57 | -0.44 |
| | ae-CC/wCVTZ | 31,431.40 | 2851.69 | 2614.48 | 0.90 | -0.40 | -0.27 |
| 8 | Semi-Experimental ^f | 34,494.31 | 3515.75 | 3202.60 | - | - | - |
| | fc-CC/VDZ | 31,020.01 | 3398.87 | 3063.23 | -10.07 [§] | -3.32 | -4.35 |
| | fc-CC/VTZ | 31,836.35 | 3492.11 | 3146.92 | -7.71 [§] | -0.67 | -1.74 |
| | fc-CC/VQZ | 31,978.63 | 3509.58 | 3162.50 | -7.29 [§] | -0.18 | -1.25 |
| | ae-CC/VDZ | 31,070.60 | 3405.23 | 3068.89 | -9.93 [§] | -3.14 | -4.18 |
| | ae-CC/VTZ | 32,080.69 | 3528.59 | 3178.94 | -7.00 [§] | 0.37 | -0.74 |
| | ae-CC/CVTZ | 31,979.91 | 3508.69 | 3161.79 | -7.29 [§] | -0.20 | -1.27 |
| | ae-CC/wCVTZ | 32,036.11 | 3514.77 | 3167.28 | -7.13 [§] | -0.03 | -1.10 |
| | ae-CC/CVQZ | 32,122.26 | 3526.79 | 3177.88 | -6.88 [§] | 0.31 | -0.77 |

^a Experimental A_0 , B_0 , and C_0 values are converted to semi-experimental A_e , B_e , and C_e values by subtracting the vibrational contributions calculated at the B3LYP/jun-cc-pVTZ level of the theory. ^b For simplicity, VnZ indicates cc-pVnZ, CVnZ indicates cc-pCVnZ, and wCVnZ indicates cc-pwCVnZ. ^c Experimental A_0 , B_0 , and C_0 values from reference [6]. ^d Experimental A_0 , B_0 , and C_0 values from reference [2]. ^e This is not a measured value. This value has been derived assuming a planar structure, that is, $1/C - 1/A - 1/B = 0$. ^f Experimental A_0 , B_0 , and C_0 values from reference [27]. [§] We note that the high percentage errors for A_e of isomers **2** and **8** are partially attributed to the B3LYP/jun-cc-pVTZ vibrational corrections used to convert the experimental A_0 rotational constant to semi-experimental equilibrium A_e value that can be compared with the CC equilibrium values.

Let us move to examining the results for the B_e and C_e rotational constants for isomer **2**. The frozen-core CC/cc-pVDZ level of the theory results in large deviations from the semi-experimental values; namely, we obtain deviations of 139 (B_e) and 145 (C_e) MHz. These translate into percentage errors of 4.0 and 4.6% relative to experiment. Moving to a

triple- ζ quality basis set reduces these errors by a factor of ~ 2 – 3 . Namely, the frozen-core CC/cc-pVTZ level of the theory results in deviations from the experiment of 55 (B_e) and 66 (C_e) MHz, which translate to percentage errors of 1.6 and 2.1%. Likewise, moving to a quadruple- ζ quality basis set further reduces these errors by a factor of ~ 3 – 4 relative to the fc-CC/cc-pVDZ level of the theory. Specifically, the frozen-core CC/cc-pVQZ level of the theory results in deviations from the experiment of 40 (B_e) and 51 (C_e) MHz. These errors translate into percentage errors that approach the 1% mark, namely, 1.1% (B_e) and 1.6% (C_e). Thus, overall the fc-CC/cc-pVnZ series ($n = D, T, Q$) exhibits a fairly monotonic basis set convergence.

Let us move to the all-electron CC calculations. Correlating the carbon 1s core electrons does not lead to a significant improvement over the poor performance of the valence CC/cc-pVDZ level of the theory (Table 1). However, correlating the core electrons in conjunction with the CC/cc-pVTZ level of the theory results in a significant improvement over the frozen-core CC/cc-pVTZ level of the theory. Specifically, the deviations between the theory and the experiments are 20 (B_e) and 34 (C_e) MHz. These deviations translate to percentage errors that are approaching or below the 1% mark, namely 0.6% (B_e) and 1.1% (C_e). However, it should be noted that the cc-pVnZ basis sets do not include polarization functions for the core electrons, and were not designed for correlated all-electron calculations. The all-electron CC/cc-pCVTZ level of the theory results in higher percentage errors of 1.2% (B_e) and $\sim 1.7\%$ (C_e) (Table 1). The weighted core-valence cc-pwCVTZ basis set, which provides a better description of core-valence correlation effects, performs slightly better than the older cc-pCVTZ basis set with percentage errors of 1.0% (B_e) and $\sim 1.5\%$ (C_e). The fact that the all-electron CC/cc-pVTZ level of the theory results in better performance than the all-electron CC/cc-pCVTZ and CC/cc-pwCVTZ levels of theory indicates that the former benefits from some degree of fortuitous error cancellations. We note that we were unable to run the all-electron CC/cc-pwCVQZ (or all-electron CC/cc-pVQZ) calculations with the computational resources available to us. However, based on the above results, we expect that the all-electron CC/cc-pwCVQZ level of the theory would provide a further improvement over the all-electron CC/cc-pwCVTZ level of the theory.

The cumulenyl isomer **3** has C_{2v} symmetry, and therefore we were able to calculate the all-electron CC rotational constants with the large cc-pCVQZ basis set (Table 1). Before discussing these results, we note that comparisons with the experiment are only made for the B_e and C_e rotational constants, since direct measurement of the A_e rotational constant is not available in the literature [2]. For the C_e rotational constant, the CC calculations in conjunction with a double- ζ quality basis set (either in conjunction with the frozen-core approximation or with all-electrons correlated) result in poor rotational constants with percentage errors of $\sim 3\%$ relative to the experiment. These results are similar to those obtained for the B_e and C_e rotational constants of isomer **2**. However, for the B_e rotational constant of isomer **3**, the CC/cc-pVDZ level of the theory (either in conjunction with the frozen-core approximation or with all-electrons correlated) results in near-zero percentage errors of 0.1–0.3%. This result is likely due to fortuitous cancellations between basis set incompleteness errors and the B3LYP/jun-cc-pVTZ vibrational corrections used to convert the experimental rotational constant to semi-experimental equilibrium values. We note that the CC/cc-pVDZ level of the theory consistently attains poor results for all other cases in Table 1. Apart from this anomaly for the B_e rotational constant of isomer **3**, the frozen core CC/cc-pVnZ series ($n = D, T, Q$) exhibits a monotonic basis-set convergence, where the percentage errors are consistently reduced when moving from the cc-pVDZ to the cc-pVTZ basis set and from the cc-pVTZ to the cc-pVQZ basis set (Table 1). Correlating all electrons at the all-electron CC/cc-pVTZ level of the theory results in a near-zero percentage error of 0.05% for the C_e rotational constant. Again, this exceptionally good agreement with the experiment is likely fortuitous, and as it the case for isomer **2**, the addition of core polarization functions in the all-electron CC/cc-pCVTZ level of the theory results in a noticeably larger percentage error of and 0.5% (C_e). The weighted core-valence cc-pwCVTZ basis set results in a similar percentage error of 0.4% for the C_e rotational constant. For the

highly symmetric **3** isomer, we were able to obtain the rotational constants at the all-electron CC/cc-pCVQZ level of the theory, which provides a significant improvement over the all-electron CC/cc-pCVTZ and CC/cc-pwCVTZ results, with percentage errors of 0.06% for the C_e rotational constant. We note that for the B_e rotational constant of isomer **3**, correlating all the electrons does not provide an improvement over the frozen-core calculations. Again, this anomalous behavior is not observed for the other isomers in Table 1.

For isomer **5**, we obtain monotonic convergence along the frozen core CC/cc-pVnZ series ($n = D, T, Q$) for the three rotational constants (A_e, B_e , and C_e). As expected, the CC/cc-pVDZ level of the theory performs poorly, with the percentage errors ranging between 2.8% (A_e) and 3.3% (B_e). The CC/cc-pVTZ level of the theory approaches or achieves percentage errors below the 1% mark; namely, the percentage errors range between 0.7% (A_e) and 1.1% (B_e). The CC/cc-pVQZ level of the theory performs well, with all percentage errors $\leq 0.4\%$. Namely, we obtain percentage errors of 0.31% (A_e), 0.44% (B_e), and 0.35% (C_e). Inspection of Table 1 reveals that correlating all electrons does not lead to an improvement over the frozen-core CC results for isomer **5**.

Isomer **8** has C_{2v} symmetry, and therefore we were able to calculate the all-electron CC rotational constants with the large cc-pCVQZ basis set (Table 1). As mentioned above, the percentage errors for the A_e rotational constant are very large, potentially due to the B3LYP/jun-cc-pVTZ vibrational corrections used to convert the experimental A_0 rotational constant to a semi-experimental equilibrium A_e value. For the B_e and C_e rotational constants, we obtain monotonic convergence along the frozen-core CC/cc-pVnZ series ($n = D, T, Q$). The CC/cc-pVQZ level of the theory performs well for the B_e rotational constant with a percentage error of 0.2%; however, for the C_e rotational constant, a relatively large percentage error of 1.2% is obtained. Correlating all electrons in the CC/cc-pCVQZ calculations results in percentage errors below the 1% mark for both rotational constants; namely, we obtain percentage errors of 0.31% (B_e) and 0.77% (C_e).

The above results show that for most of the rotational constants, the fc-CC/cc-pVnZ series ($n = D, T, Q$) exhibits a fairly monotonic basis set convergence and that the CC/cc-pVTZ level of the theory (in conjunction with the frozen-core approximation or with all electrons correlated) results in percentage errors approaching or below the 1% mark. However, for a subset of the rotational constants (namely, A_e of isomers **2** and **8**, and B_e of isomer **3**), very large percentage errors above 3% are obtained, potentially due to the B3LYP/jun-cc-pVTZ vibrational corrections used to convert the experimental rotational constant to semi-experimental equilibrium values that can be compared with the CC results. Additional factors that could affect the above percentage errors are the complete neglect of anharmonicity and post-CC effects, as well as issues associated with inaccurate geometries. To isolate the effects of basis set size and correlating the core electrons at the CC level, it is instructive to compare the fc-CC and ae-CC levels to the best available level of the theory in Table 1. These results are presented in Table 2. The frozen-core CC/cc-pVDZ attains large percentage errors of $\sim 3\%$ in nearly all cases. Correlating all electrons does not lead to a performance improvement at this level of the theory. The frozen-core CC/cc-pVTZ results in significantly better performance with nearly all percentage errors $\leq 0.5\%$. The two exceptions to this are the A_e rotational constant of isomer **2** with a percentage error of 0.8% and the B_e rotational constant of isomer **5** with a percentage error of 0.6%. Here, correlating all electrons does lead to an improvement in performance, with the notable exception of the A_e rotational constant of isomer **5**. Using the cc-pCVTZ or cc-pwCVTZ basis sets in the ae-CC calculations does not lead to an improvement in performance over the cc-pVTZ basis set, indicating that the latter benefits from some degree of fortuitous error cancellation.

Table 2. Percentage errors in theoretical equilibrium rotational constants (A_e , B_e , C_e) for isomers 2, 3, 5, and 8 obtained at the CC level using different basis sets (with and without the frozen-core approximation) relative to the highest level of the theory in Table 1.

| Isomer | Level of the Theory ^a | % Error | | |
|--------|----------------------------------|---------|-------|-------|
| | | A_e | B_e | C_e |
| 2 | fc-CC/VDZ ^b | −4.16 | −2.92 | −3.03 |
| | fc-CC/VTZ ^b | −0.81 | −0.44 | −0.47 |
| | ae-CC/VDZ ^c | −3.94 | −2.89 | −2.98 |
| | ae-CC/VTZ ^c | 0.28 | 0.44 | 0.43 |
| | ae-CC/CVTZ ^c | −0.23 | −0.16 | −0.16 |
| 3 | fc-CC/VDZ ^b | −2.66 | −3.08 | −3.08 |
| | fc-CC/VTZ ^b | −0.11 | −0.42 | −0.42 |
| | ae-CC/VDZ ^d | −2.77 | −3.36 | −3.35 |
| | ae-CC/VTZ ^d | 0.44 | 0.11 | 0.11 |
| | ae-CC/CVTZ ^d | −0.18 | −0.46 | −0.46 |
| | ae-CC/wCVTZ ^d | −0.10 | −0.31 | −0.31 |
| 5 | fc-CC/VDZ ^b | −3.09 | −2.86 | −2.88 |
| | fc-CC/VTZ ^b | 0.37 | −0.63 | −0.55 |
| | ae-CC/VDZ ^c | −3.53 | −2.72 | −2.79 |
| | ae-CC/VTZ ^c | 3.30 | −0.32 | −0.03 |
| | ae-CC/CVTZ ^c | −0.09 | −0.17 | −0.17 |
| 8 | fc-CC/VDZ ^b | −3.00 | −3.15 | −3.14 |
| | fc-CC/VTZ ^b | −0.44 | −0.50 | −0.49 |
| | ae-CC/VDZ ^d | −3.27 | −3.45 | −3.43 |
| | ae-CC/VTZ ^d | −0.13 | 0.05 | 0.03 |
| | ae-CC/CVTZ ^d | −0.44 | −0.51 | −0.51 |
| | ae-CC/wCVTZ ^d | −0.27 | −0.34 | −0.33 |

^a For simplicity, VnZ indicates cc-p VnZ , $CVnZ$ indicates cc-p $CVnZ$, and $wCVnZ$ indicates cc-pw $CVnZ$. ^b Percentage errors are calculated relative to the fc-CC/cc-pVQZ level of the theory. ^c Percentage errors are calculated relative to the ae-CC/cc-pwCVTZ level of the theory. ^d Percentage errors are calculated relative to the ae-CC/cc-pCVQZ level of the theory.

We now focus our attention on the comparison of rotational constants calculated using various DFT methods across the rungs of Jacob's Ladder [83]. We also refer the reader to several related benchmark studies which considered other species [84–87]. We will primarily compare the DFT results to the best level of the theory in Table 1, namely ae-CC/cc-pwCVTZ for isomers 2 and 5, and ae-CC/cc-pCVQZ for isomers 3 and 8 (for a comparison between the DFT results and the semi-experimental values, see the Supplementary Materials). The DFT rotational constants, the deviations from our best CC values, and the percentage errors are given in Table 3. In the following discussion, we will focus on functionals that are able to consistently achieve percentage errors from CC below 1% across all isomers (2, 3, 5, and 8) and rotational constants (A_e , B_e , and C_e). Let us begin with several general observations. The two range-separated hybrid functionals CAM-B3LYP-D3BJ and ω B97X-D show poor performance and cannot achieve this goal. The global hybrid functionals B3LYP-D3BJ and PBE0-D3 show better performance and result in percentage errors approaching (or below) 1% for the B_e and C_e rotational constants for all isomers but not for the A_e rotational constants. We, therefore, do not recommend the use of these range-separated and global hybrid functionals for the calculation of rotational constants in similar systems. Moving to the hybrid-meta generalized gradient approximation (GGA) methods from rung 4 of Jacob's Ladder, BMK-D3BJ shows improved performance relative to M06-2X. In particular, BMK-D3BJ results in percentage errors $\leq 1.0\%$ for all but two rotational constants. The two rotational constants for which the percentage error is 1.3% are B_e and C_e of isomer 5. However, as we shall see below, BMK-D3BJ does not provide a significant improvement over the lower-level GGA and meta-GGA methods. The M06-2X

method results in percentage errors $\leq 1.0\%$ for only four rotational constants (A_e of isomer 3 and all rotational constants of isomer 8).

Table 3. Theoretical equilibrium rotational constants (A_e , B_e , C_e ; in MHz) obtained using DFT methods across the rungs of Jacob's Ladder. These results are compared to the best CC results from Table 1 for Isomers 2, 3, 5, and 8.

| Isomer | Level of the Theory | Rotational Constants | | | % Error | | |
|----------------|---------------------|----------------------|---------|---------|---------|-------|-------|
| | | A_e | B_e | C_e | A_e | B_e | C_e |
| 2 ^a | PBE-D3BJ | 34,776.97 | 3410.3 | 3105.75 | 0.67 | −0.11 | −0.04 |
| | BLYP-D3BJ | 34,772.95 | 3406.65 | 3102.68 | 0.66 | −0.22 | −0.14 |
| | TPSS-D3BJ | 34,832.08 | 3421.18 | 3115.2 | 0.83 | 0.21 | 0.27 |
| | BMK-D3BJ | 34,305.88 | 3417.45 | 3107.86 | −0.69 | 0.10 | 0.03 |
| | B2-PLYP-D3BJ | 35,080.47 | 3437.28 | 3130.54 | 1.55 | 0.68 | 0.76 |
| | DSD-PBEP86-D3BJ | 34,906.49 | 3425.77 | 3119.61 | 1.05 | 0.34 | 0.41 |
| 3 ^b | PBE-D3BJ | 288,084.24 | 2289.71 | 2271.66 | −1.04 | −0.46 | −0.46 |
| | BLYP-D3BJ | 290,215.02 | 2292.37 | 2274.41 | −0.31 | −0.35 | −0.34 |
| | TPSS-D3BJ | 291,046.32 | 2299.95 | 2281.92 | −0.02 | −0.02 | −0.02 |
| | BMK-D3BJ | 290,741.94 | 2324.26 | 2305.82 | −0.13 | 1.04 | 1.03 |
| | B2-PLYP-D3BJ | 293,012.38 | 2313.86 | 2295.74 | 0.65 | 0.59 | 0.59 |
| | DSD-PBEP86-D3BJ | 291,090.37 | 2305.76 | 2287.64 | −0.01 | 0.24 | 0.24 |
| 5 ^a | PBE-D3BJ | 31,828.92 | 2844.85 | 2611.44 | 1.26 | −0.24 | −0.12 |
| | BLYP-D3BJ | 31,858.95 | 2844.08 | 2610.99 | 1.36 | −0.27 | −0.13 |
| | TPSS-D3BJ | 31,747.91 | 2858.87 | 2622.7 | 1.01 | 0.25 | 0.31 |
| | BMK-D3BJ | 31,631.84 | 2889.51 | 2647.65 | 0.64 | 1.33 | 1.27 |
| | B2-PLYP-D3BJ | 31,903.2 | 2873.29 | 2635.89 | 1.50 | 0.76 | 0.82 |
| | DSD-PBEP86-D3BJ | 31,573.48 | 2867.58 | 2628.82 | 0.45 | 0.56 | 0.55 |
| 8 ^b | PBE-D3BJ | 31,895.1 | 3495.39 | 3150.17 | −0.71 | −0.89 | −0.87 |
| | BLYP-D3BJ | 31,951.11 | 3492.37 | 3148.26 | −0.53 | −0.98 | −0.93 |
| | TPSS-D3BJ | 32,043.94 | 3507.76 | 3161.66 | −0.24 | −0.54 | −0.51 |
| | BMK-D3BJ | 31,945.51 | 3514.9 | 3166.5 | −0.55 | −0.34 | −0.36 |
| | B2-PLYP-D3BJ | 32,223.32 | 3538.94 | 3188.73 | 0.31 | 0.34 | 0.34 |
| | DSD-PBEP86-D3BJ | 32,086.32 | 3531.32 | 3181.2 | −0.11 | 0.13 | 0.10 |

^a Percentage errors are calculated relative to the ae-CC/cc-pwCVTZ level of the theory. ^b Percentage errors are calculated relative to the ae-CC/cc-pCVQZ level of the theory.

Let us move to the pure DFT methods from rungs 2 and 3 of Jacob's Ladder. Both GGA methods BLYP-D3BJ and PBE-D3BJ result in percentage errors from CC below 1% across nearly all isomers and rotational constants. This is indeed remarkable, considering that the hybrid GGA methods were unable to achieve this goal. In particular, BLYP-D3BJ attains percentage errors $\leq 0.7\%$ for all but three rotational constants (Table 3). Similarly, PBE-D3BJ attains percentage errors $\leq 0.7\%$ for all but four rotational constants. Let us move to the performance of the meta-GGA methods, which additionally employ the kinetic energy density. The highly empirical M06-L method results in poor performance with percentage errors $\geq 1\%$ for half of the rotational constants. However, the non-empirical TPSS meta-GGA functional results in exceptional performance, with practically all percentage errors being below 0.6%. Furthermore, with the exception of two additional rotational constants (B_e and C_e for isomer 8), TPSS-D3BJ results in percentage errors being below 0.3%.

Let us move on to the double-hybrid DFT methods, which involve both Hartree-Fock exchange and MP2-like correlation from second-order Møller-Plesset perturbation theory. The older generation B2-PLYP functional shows good performance with nearly all percentage errors below 0.8%. However, it should be noted that overall, the meta-GGA TPSS-D3BJ method provides better performance than B2-PLYP. The DSD-PBEP86-D3BJ functional in which the same-spin and opposite-spin components of the correlation energy are scaled by empirically motivated scaling factors achieves significantly better performance than B2-PLYP. Namely, with the exception of A_e for isomer 2 and B_e for isomer 5, all the percentage errors for DSD-PBEP86 are below 0.5%. Furthermore, for half of the rotational constants, the percentage errors are below the 0.2% mark. Together with previous

findings [84–86,88,89], these results place DSD-PBEP86-D3BJ as an excellent functional for the prediction of geometrical and spectroscopic properties. However, we note that this excellent performance comes with a significant increase in the computational cost. Whereas the computational cost of the TPSS method, which is the second-best performer, scales as $\sim N_{bas}^3$ with respect to the number of basis functions, DSD-PBEP86 calculations scale as $\sim N_{bas}^5$. Still, DSD-PBEP86 calculations are computationally far more economical than CC calculations, which scale as $\sim N_{bas}^7$ [54]. Overall, we would recommend using DSD-PBEP86-D3BJ for relatively small systems, such as those considered in the present work, and TPSS-D3BJ for significantly larger systems.

So far, we have discussed the performance of the isomers **2**, **3**, **5**, and **8**, which have been synthesized in the lab, and for which experimental rotational constants have been measured. We have examined the performance of the CC method in conjunction with a variety of basis sets and treatment of the core electrons, and also identified the DFT methods, which are able to systematically reproduce the best CC rotational constants with percentage errors below the 1% mark. It is of interest to use these accurate CC and DFT methods for calculating the rotational constants of the isomers for which experimental data are not available. These results are given in Table 4. Both isomers **4** and **6** could be considered acetylenic carbenes from the electronic structure point of view, which are well-known intermediates in many prototypical organic reactions [22,90,91]. It is noted here that isomers **4**, **6**, and **9** may have been overlooked in previous experimental and theoretical studies [2,3,21]. On the contrary, isomers **11** and **13** have been considered in previous theoretical studies, as they contain the unconventional planar tetracoordinate carbon atoms [92,93]. Nevertheless, the rotational constants have not been reported in these studies, and the focus was rather related to the chemical bonding aspects of these molecules. It is noted here that **7** is a second-order saddle point, whereas **10** and **15** are transition states. It is also noted here that isomers **11** and **12** lack permanent dipole moments due to symmetry, and thus they are not suitable candidates for FTMW spectroscopy. We note that the geometry of **4** rearranges to **6** at the fc-CC/cc-pVDZ level of the theory, indicating that cc-pVDZ basis set is not adequate for these fluxional molecules. Also, for **4**, the A_e rotational constant value obtained at the TPSS-D3BJ/cc-pVQZ level seems to be problematic, as the equilibrium geometry nearly rearranges to **6**. In addition, although the B_e and C_e rotational constants are consistent between DSD-PBEP86 and ae-CC methods for **6**, the A_e rotational constant value is inconsistent between these methods. Therefore, unless these molecules are experimentally identified in the laboratory and rotational constants are measured, it is difficult to reach a conclusion as far as which method is most accurate. However, such issues seem to disappear for isomers **9** and **13**, as they are not fluxional molecules like **4** and **6**. Therefore, for **9** and **13** one could rely on the values obtained from ae-CC/cc-pVQZ and DSD-PBEP86/cc-pVQZ levels.

Table 4. Theoretically calculated rotational constants (in MHz) of unknown C_5H_2 isomers at different CC and DFT levels.

| Isomer | Level of the Theory ^a | A_e | B_e | C_e |
|----------|----------------------------------|------------|---------|---------|
| 4 | fc-CC/VTZ | 44,468.31 | 2675.36 | 2523.54 |
| | fc-CC/VQZ | 44,559.66 | 2687.42 | 2534.56 |
| | ae-CC/VTZ | 47,663.99 | 2670.19 | 2528.54 |
| | ae-CC/CVTZ | 44,964.29 | 2683.13 | 2532.04 |
| | ae-CC/wCVTZ | 45,248.67 | 2684.92 | 2534.53 |
| | ae-CC/CVQZ | 45,285.14 | 2693.43 | 2542.23 |
| | TPSS-D3BJ/VQZ | 415,092.95 | 2314.94 | 2302.10 |
| | DSD-PBEP86-D3BJ/VQZ | 48,334.30 | 2669.57 | 2529.84 |

Table 4. Cont.

| Isomer | Level of the Theory ^a | A_e | B_e | C_e |
|---------------------|----------------------------------|------------|---------|---------|
| 6 | fc-CC/VTZ | 575,100.98 | 2265.22 | 2256.33 |
| | fc-CC/VQZ | 599,411.76 | 2273.66 | 2265.06 |
| | ae-CC/VTZ | 611,557.40 | 2287.33 | 2278.81 |
| | ae-CC/CVTZ | 572,323.22 | 2274.94 | 2265.93 |
| | ae-CC/wCVTZ | 526,553.84 | 2282.03 | 2272.19 |
| | TPSS-D3BJ/VQZ | 413,454.77 | 2315.19 | 2302.29 |
| | DSD-PBEP86-D3BJ/VQZ | 672,216.98 | 2287.43 | 2279.67 |
| 9 | fc-CC/VTZ | 31,658.89 | 4569.62 | 3993.24 |
| | fc-CC/VQZ | 31,908.98 | 4592.16 | 4014.43 |
| | ae-CC/VTZ | 32,178.66 | 4612.32 | 4034.09 |
| | ae-CC/CVTZ | 31,919.04 | 4589.89 | 4012.85 |
| | ae-CC/wCVTZ | 32,008.12 | 4598.06 | 4020.50 |
| | ae-CC/CVQZ | 32,169.05 | 4612.09 | 4033.77 |
| | TPSS-D3BJ/VQZ | 32,428.41 | 4572.42 | 4007.38 |
| DSD-PBEP86-D3BJ/VQZ | 32,191.22 | 4616.16 | 4037.23 | |
| 13 | fc-CC/VTZ | 18,897.05 | 5445.32 | 4227.22 |
| | fc-CC/VQZ | 19,024.44 | 5480.23 | 4254.63 |
| | ae-CC/VTZ | 19,101.44 | 5510.40 | 4276.67 |
| | ae-CC/CVTZ | 19,000.57 | 5475.68 | 4250.69 |
| | ae-CC/wCVTZ | 19,043.27 | 5484.32 | 4258.03 |
| | ae-CC/CVQZ | 19,130.16 | 5509.91 | 4277.81 |
| | TPSS-D3BJ/VQZ | 19,008.80 | 5482.72 | 4255.35 |
| DSD-PBEP86-D3BJ/VQZ | 19,144.14 | 5535.55 | 4293.95 | |

^a For simplicity, VnZ indicates cc-pVnZ, $CVnZ$ indicates cc-pCVnZ, and $wCVnZ$ indicates cc-pwCVnZ.

4. Conclusions

This work considers a series of challenging carbene C_5H_2 isomers with cumulene, acetylene, or strained cyclopropene moieties to examine the theoretical rotational constants predicted by frozen-core and all-electron CCSD(T) calculations, as well as a range of DFT methods. The considered C_5H_2 isomers (**2**, **3**, **5**, and **8**) have been experimentally identified using FTMW spectroscopy, and two of them (**2** and **3**) have been recently confirmed in the interstellar medium. The calculated rotational constants are compared to semi-experimental rotational constants obtained by converting the vibrationally averaged experimental rotational constants (A_0 , B_0 , and C_0) to equilibrium values by subtracting the vibrational contributions (calculated at the B3LYP/jun-cc-pVTZ level of the theory). We find that calculating the equilibrium rotational constants of these C_5H_2 isomers is a difficult task, even at the CCSD(T) level. For example, at the all-electron CCSD(T)/cc-pwCVTZ level of the theory, we obtain percentage errors $\leq 0.4\%$ (C_e of isomer **3**, B_e and C_e of isomer **5**, and B_e of isomer **8**) and 0.9–1.5% (B_e and C_e of isomer **2**, A_e of isomer **5**, and C_e of isomer **8**), whereas for the A_e rotational constant of isomers **2** and **8** and B_e rotational constant of isomer **3**, high percentage errors above 3% are obtained. These results highlight the challenges associated with calculating accurate rotational constants for isomers with highly challenging electronic structures, which is further complicated by the need to convert vibrationally averaged experimental rotational constants to equilibrium values. We use our best CCSD(T) rotational constants (namely, ae-CCSD(T)/cc-pwCVTZ for isomers **2** and **5**, and ae-CCSD(T)/cc-pCVQZ for isomers **3** and **8**) to evaluate the performance of DFT methods across the rungs of Jacob's Ladder. We find that the considered pure functionals (BLYP-D3BJ, PBE-D3BJ, and TPSS-D3BJ) perform significantly better than the global and range-separated hybrid functionals. The double-hybrid DSD-PBEP86-D3BJ method shows the best overall performance with percentage errors below 0.5% in nearly all cases. Therefore, we recommend the use of the DSD-PBEP86-D3BJ method for relatively small systems, whereas for larger systems, the TPSS-D3BJ method is recommended. We hope that these results will help identify the unknown isomers (**4**, **6**, **9**, **13**) in the laboratory and, consequently, in the interstellar medium.

Supplementary Materials: The following supporting information can be downloaded at: <https://www.mdpi.com/article/10.3390/molecules28186537/s1>.

Author Contributions: Conceptualization, V.S.T. and A.K.; methodology, A.K. and V.S.T.; software, A.K. and V.S.T.; validation, V.S.T. and A.K.; formal analysis, V.S.T. and A.K.; investigation, V.S.T. and A.K.; resources, A.K. and V.S.T.; data curation, A.K. and V.S.T.; writing—original draft preparation, V.S.T. and A.K.; writing—review and editing, V.S.T. and A.K.; visualization, V.S.T.; supervision, V.S.T.; project administration, V.S.T. All authors have read and agreed to the published version of the manuscript.

Funding: Computational support provided at the SDSU (for VST) by DURIP Grant W911NF-10-1-0157 from the U.S. Department of Defense and by NSF CRIF 338 Grant CHE-0947087 is gratefully acknowledged.

Informed Consent Statement: Not applicable

Acknowledgments: This research work in part was undertaken with the assistance of resources and services from the National Computational Infrastructure (NCI), which is supported by the Australian Government. V.S.T. thanks Andrew L. Cooksy (SDSU, San Diego) for providing additional computing time.

Conflicts of Interest: The authors declare no conflicts of interest.

Sample Availability: Not applicable

Abbreviations

The following abbreviations are used in this manuscript:

| | |
|-----|--|
| DFT | Density functional theory |
| CC | CCSD(T), coupled-cluster singles, doubles including perturbative triples |
| ptC | Planar tetracoordinate carbon |

References

1. Ekkers, J.; Flygare, W.H. Pulsed microwave Fourier transform spectrometer. *Rev. Sci. Instruments* **1976**, *47*, 448–454. [[CrossRef](#)]
2. McCarthy, M.C.; Travers, M.J.; Kovács, A.; Chen, W.; Novick, S.E.; Gottlieb, C.A.; Thaddeus, P. Detection and Characterization of the Cumulene Carbenes H_2C_5 and H_2C_6 . *Science* **1997**, *275*, 518–520. [[CrossRef](#)]
3. Seburg, R.A.; McMahon, R.J.; Stanton, J.F.; Gauss, J. Structures and Stabilities of C_5H_2 Isomers: Quantum Chemical Studies. *J. Am. Chem. Soc.* **1997**, *119*, 10838–10845. [[CrossRef](#)]
4. Sattelmeyer, K.W.; Stanton, J.F. Computational Studies of C_6H_2 Isomers. *J. Am. Chem. Soc.* **2000**, *122*, 8220–8227. [[CrossRef](#)]
5. McCarthy, M.C.; Thaddeus, P. Laboratory Detection of a Bent-Chain Carbene Isomer of C_6H_2 . *Astrophys. J. Lett.* **2002**, *569*, L55. [[CrossRef](#)]
6. Travers, M.J.; McCarthy, M.C.; Gottlieb, C.A.; Thaddeus, P. Laboratory Detection of the Ring-Chain Molecule C_5H_2 . *Astrophys. J.* **1997**, *483*, L135–L138. [[CrossRef](#)]
7. Thirumoorthy, K.; Viji, M.; Pandey, A.P.; Netke, T.G.; Sekar, B.; Yadav, G.; Deshpande, S.; Thimmakondur, V.S. Many Unknowns Below or Close to the Experimentally Known Cumulene Carbene—A Case Study of C_9H_2 Isomers. *Chem. Phys.* **2019**, *527*, 110496. [[CrossRef](#)]
8. Thirumoorthy, K.; Cooksy, A.; Thimmakondur, V.S. $Si_2C_5H_2$ Isomers—Search Algorithms Versus Chemical Intuition. *Phys. Chem. Chem. Phys.* **2020**, *22*, 5865–5872. [[CrossRef](#)]
9. Watrous, A.G.; Westbrook, B.R.; Fortenberry, R.C. Theoretical spectra and energetics for $c-C_3HC_2H$, $l-C_5H_2$, and bipyramidal D_{3h} C_5H_2 . *Front. Astron. Space Sci.* **2022**, *9*, 1051535. [[CrossRef](#)]
10. Roy, T.; Ghosal, S.; Thimmakondur, V.S. Six Low-Lying Isomers of $C_{11}H_8$ Are Unidentified in the Laboratory—A Theoretical Study. *J. Phys. Chem. A* **2021**, *125*, 4352–4364. [[CrossRef](#)] [[PubMed](#)]
11. Hansen, C.S.; Peeters, E.; Cami, J.; Schmidt, T.W. Open questions on carbon-based molecules in space. *Commun. Chem.* **2022**, *5*, 94. [[CrossRef](#)]
12. Vega-Vega, A.; Largo, A.; Redondo, P.; Barrientos, C. Structure and Spectroscopic Properties of [Mg,C,N,O] Isomers: Plausible Astronomical Molecules. *ACS Earth Space Chem.* **2017**, *1*, 158–167. [[CrossRef](#)]
13. Tuli, L.B.; Goettl, S.J.; Turner, A.M.; Howlader, A.H.; Hemberger, P.; Wnuk, S.F.; Guo, T.; Mebel, A.M.; Kaiser, R.I. Gas phase synthesis of the C_{40} nano bowl $C_{40}H_{10}$. *Nat. Commun.* **2023**, *14*, 1527. [[CrossRef](#)]
14. Thimmakondur, V.S.; Karton, A. Energetic and Spectroscopic Properties of the Low-Lying C_7H_2 Isomers: A High-Level Ab Initio Perspective. *Phys. Chem. Chem. Phys.* **2017**, *19*, 17685–17697. [[CrossRef](#)]

15. Thirumoorthy, K.; Karton, A.; Thimmakonda, V.S. From High-Energy C₇H₂ Isomers with A Planar Tetracoordinate Carbon Atom to An Experimentally Known Carbene. *J. Phys. Chem. A* **2018**, *122*, 9054–9064. [[CrossRef](#)] [[PubMed](#)]
16. Panda, S.; Sivadasan, D.; Job, N.; Sinjari, A.; Thirumoorthy, K.; Anoop, A.; Thimmakonda, V.S. Why Are MgC₃H Isomers Missing in the Interstellar Medium? *J. Phys. Chem. A* **2022**, *126*, 4465–4475. [[CrossRef](#)]
17. Puzzarini, C.; Heckert, M.; Gauss, J. The Accuracy of Rotational Constants Predicted by High-Level Quantum-Chemical Calculations. I. Molecules Containing First-Row Atoms. *J. Chem. Phys.* **2008**, *128*, 194108. [[CrossRef](#)] [[PubMed](#)]
18. Puzzarini, C.; Stanton, J.F.; Gauss, J. Quantum-Chemical Calculation of Spectroscopic Parameters for Rotational Spectroscopy. *Int. Rev. Phys. Chem.* **2010**, *29*, 273–367. [[CrossRef](#)]
19. Puzzarini, C.; Stanton, J.F. Connections between the accuracy of rotational constants and equilibrium molecular structures. *Phys. Chem. Chem. Phys.* **2023**, *25*, 1421–1429. [[CrossRef](#)] [[PubMed](#)]
20. Fulara, J.; Freivogel, P.; Forney, D.; Maier, J.P. Electronic Absorption Spectra of Linear Carbon Chains in Neon Matrices. III. HC_{2n+1}H. *J. Chem. Phys.* **1995**, *103*, 8805–8810. [[CrossRef](#)]
21. Blanksby, S.J.; Dua, S.; Bowie, J.H.; Schröder, D.; Schwarz, H. Gas-Phase Syntheses of Three Isomeric C₅H₂ Radical Anions and Their Elusive Neutrals. A Joint Experimental and Theoretical Study. *J. Phys. Chem. A* **1998**, *102*, 9949–9956. [[CrossRef](#)]
22. Bowling, N.P.; Halter, R.J.; Hodges, J.A.; Seburg, R.A.; Thomas, P.S.; Simmons, C.S.; Stanton, J.F.; McMahon, R.J. Reactive Carbon-Chain Molecules: Synthesis of 1-Diazo-2,4-pentadiyne and Spectroscopic Characterization of Triplet Pentadiynylidene (H-C-C- \dot{C} -C-H). *J. Am. Chem. Soc.* **2006**, *128*, 3291–3302. [[CrossRef](#)]
23. Sun, Y.L.; Huang, W.J.; Lee, S.H. Formation of C₃H₂, C₅H₂, C₇H₂, and C₉H₂ From Reactions of CH, C₃H, C₅H, and C₇H Radicals with C₂H₂. *Phys. Chem. Chem. Phys.* **2016**, *18*, 2120–2129. [[CrossRef](#)] [[PubMed](#)]
24. Steglich, M.; Fulara, J.; Maity, S.; Nagy, A.; Maier, J.P. Electronic Spectra of Linear HC₅H and Cumulene Carbene H₂C₅. *J. Chem. Phys.* **2015**, *142*, 244311. [[CrossRef](#)]
25. Reusch, E.; Kaiser, D.; Schleier, D.; Buschmann, R.; Krueger, A.; Hermann, T.; Engels, B.; Fischer, I.; Hemberger, P. Pentadiynylidene and Its Methyl-Substituted Derivates: Threshold Photoelectron Spectroscopy of R₁-C₅-R₂ Triplet Carbon Chains. *J. Phys. Chem. A* **2019**, *123*, 2008–2017. [[CrossRef](#)]
26. He, C.; Galimova, G.R.; Luo, Y.; Zhao, L.; Eckhardt, A.K.; Sun, R.; Mebel, A.M.; Kaiser, R.I. A Chemical Dynamics Study on the Gas-Phase Formation of Triplet and Singlet C₅H₂ Carbenes. *Proc. Natl. Acad. Sci. USA* **2020**, *117*, 30142–30150. [[CrossRef](#)]
27. Gottlieb, C.A.; McCarthy, M.C.; Gordon, V.D.; Chakan, J.M.; Apponi, A.J.; Thaddeus, P. Laboratory Detection of Two New C₅H₂ Isomers. *Astrophys. J.* **1998**, *509*, L141. [[CrossRef](#)]
28. Thaddeus, P.; Vrtilik, J.M.; Gottlieb, C.A. Laboratory and Astronomical Identification of Cyclopropenylidene, C₃H₂. *Astrophys. J.* **1985**, *299*, L63–L66. [[CrossRef](#)]
29. Cernicharo, J.; Gottlieb, C.A.; Guelin, M.; Killian, T.C.; Paubert, G.; Thaddeus, P.; Vrtilik, J.M. Astronomical Detection of H₂CCC. *Astrophys. J.* **1991**, *368*, L39–L41. [[CrossRef](#)]
30. Vrtilik, J.M.; Gottlieb, C.A.; Gottlieb, E.W.; Killian, T.C.; Thaddeus, P. Laboratory Detection of Propadienylidene, H₂CCC. *Astrophys. J.* **1990**, *364*, L53–L56. [[CrossRef](#)]
31. Spezzano, S.; Brünken, S.; Schilke, P.; Caselli, P.; Menten, K.M.; McCarthy, M.C.; Bizzocchi, L.; Treviño-Morales, S.P.; Aikawa, Y.; Schlemmer, S. Interstellar Detection of c-C₃D₂. *Astrophys. J.* **2013**, *769*, L19. [[CrossRef](#)]
32. Sipilä, O.; Spezzano, S.; Caselli, P. Understanding the C₃H₂ Cyclic-to-Linear Ratio in L1544. *Astron. Astrophys.* **2016**, *591*, L1. [[CrossRef](#)]
33. Spezzano, S.; Caselli, P.; Bizzocchi, L.; Giuliano, B.M.; Lattanzi, V. The Observed Chemical Structure of L1544. *Astron. Astrophys.* **2017**, *606*, A82. [[CrossRef](#)]
34. Chantzos, J.; Spezzano, S.; Caselli, P.; Chacón-Tanarro, A.; Bizzocchi, L.; Sipilä, O.; Giuliano, B.M. A Study of the c-C₃HD/c-C₃H₂ Ratio in Low-mass Star-forming Regions. *Astrophys. J.* **2018**, *863*, 126. [[CrossRef](#)]
35. Cabezas, C.; Tercero, B.; Agúndez, M.; Marcelino, N.; Pardo, J.R.; de Vicente, P.; Cernicharo, J. Cumulene Carbenes in TMC-1: Astronomical Discovery of 1-H₂C₅. *Astron. Astrophys.* **2021**, *650*, L9. [[CrossRef](#)]
36. Cernicharo, J.; Agúndez, M.; Cabezas, C.; Tercero, B.; Marcelino, N.; Pardo, J.R.; de Vicente, P. Pure Hydrocarbon Cycles in TMC-1: Discovery of Ethynyl Cyclopropenylidene, Cyclopentadiene, and Indene. *Astron. Astrophys.* **2021**, *649*, L15. [[CrossRef](#)]
37. Mebel, A.M.; Kim, G.S.; Kislov, V.V.; Kaiser, R.I. The Reaction of Tricarbon with Acetylene: An Ab Initio/RRKM Study of the Potential Energy Surface and Product Branching Ratios. *J. Phys. Chem. A* **2007**, *111*, 6704–6712. [[CrossRef](#)] [[PubMed](#)]
38. Gu, X.; Guo, Y.; Mebel, A.M.; Kaiser, R.I. A Crossed Beam Investigation of the Reactions of Tricarbon Molecules, C₃($\tilde{X}^1\Sigma_g^+$), with Acetylene, C₂H₂($\tilde{X}^1\Sigma_g^+$), Ethylene, C₂H₄(\tilde{X}^1A_g), and Benzene, C₆H₆(\tilde{X}^1A_{1g}). *Chem. Phys. Lett.* **2007**, *449*, 44–52. [[CrossRef](#)]
39. Sun, B.J.; Huang, C.Y.; Kuo, H.H.; Chen, K.T.; Sun, H.L.; Huang, C.H.; Tsai, M.F.; Kao, C.H.; Wang, Y.S.; Gao, L.G.; et al. Formation of Interstellar 2,4-pentadiynylidyne, HCCCCC(X²Π), via the Neutral-Neutral Reaction of Ground State Carbon Atom, C(³P), with Diacetylene, HCCCCH($\tilde{X}^1\Sigma_g^+$). *J. Chem. Phys.* **2008**, *128*, 244303. [[CrossRef](#)]
40. Hansen, N.; Klippenstein, S.J.; Miller, J.A.; Wang, J.; Cool, T.A.; Law, M.E.; Westmoreland, P.R.; Kasper, T.; Kohse-Höinghaus, K. Identification of C₅H_x Isomers in Fuel-Rich Flames by Photoionization Mass Spectrometry and Electronic Structure Calculations. *J. Phys. Chem. A* **2006**, *110*, 4376–4388. [[CrossRef](#)] [[PubMed](#)]
41. Thimmakonda, V.S.; Karton, A. The Quest for the Carbene Bent-pentadiynylidene Isomer of C₅H₂. *Chem. Phys.* **2018**, *515*, 411–417. [[CrossRef](#)]

42. Thimmakonda, V.S.; Ulusoy, I.; Wilson, A.K.; Karton, A. Theoretical Studies of Two Key Low-Lying Carbenes of C₅H₂ Missing in the Laboratory. *J. Phys. Chem. A* **2019**, *123*, 6618–6627. [[CrossRef](#)] [[PubMed](#)]
43. Karton, A.; Thimmakonda, V.S. From Molecules with a Planar Tetracoordinate Carbon to an Astronomically Known C₅H₂ Carbene. *J. Phys. Chem. A* **2022**, *126*, 2561–2568. [[CrossRef](#)]
44. Fortenberry, R.C. The Formation of Astromolecule Ethynyl Cyclopropenylidene (c-C₃HCCH) from C₂H and c-C₃H₂. *Astrophys. J.* **2021**, *921*, 132. [[CrossRef](#)]
45. Thimmakonda, V.S.; Thirumoorthy, K. Si₃C₂H₂ Isomers with A Planar Tetracoordinate Carbon or Silicon Atom(s). *Comput. Theor. Chem.* **2019**, *1157*, 40–46. [[CrossRef](#)]
46. Thirumoorthy, K.; Chandrasekaran, V.; Cooksy, A.L.; Thimmakonda, V.S. Kinetic Stability of Si₂C₅H₂ Isomer with a Planar Tetracoordinate Carbon Atom. *Chemistry* **2021**, *3*, 13–27. [[CrossRef](#)]
47. Thirumoorthy, K.; Thimmakonda, V.S. Flat Crown Ethers with Planar Tetracoordinate Carbon Atoms. *Int. J. Quantum Chem.* **2021**, *121*, e26479. [[CrossRef](#)]
48. Job, N.; Khatun, M.; Thirumoorthy, K.; CH, S.S.R.; Chandrasekaran, V.; Anoop, A.; Thimmakonda, V.S. CAI₄Mg^{0/−}: Global Minima with a Planar Tetracoordinate Carbon Atom. *Atoms* **2021**, *9*, 24. [[CrossRef](#)]
49. Satpati, S.; Roy, T.; Giri, S.; Anoop, A.; Thimmakonda, V.S.; Ghosal, S. Structure and Bonding Patterns in C₅H₄ Isomers: Pyramidane, Planar Tetracoordinate Carbon, and Spiro Molecules. *Atoms* **2023**, *11*, 96. [[CrossRef](#)]
50. Raghavachari, K.; Trucks, G.W.; Pople, J.A.; Head-Gordon, M. A Fifth-Order Perturbation Comparison of Electron Correlation Theories. *Chem. Phys. Lett.* **1989**, *157*, 479–483. [[CrossRef](#)]
51. Bartlett, R.J.; Watts, J.; Kucharski, S.; Noga, J. Non-Iterative Fifth-Order Triple and Quadruple Excitation Energy Corrections in Correlated Methods. *Chem. Phys. Lett.* **1990**, *165*, 513–522. [[CrossRef](#)]
52. Stanton, J.F. Why CCSD(T) Works: A Different Perspective. *Chem. Phys. Lett.* **1997**, *281*, 130–134. [[CrossRef](#)]
53. K., R. Historical perspective on: A fifthorder perturbation comparison of electron correlation theories [Volume 157, Issue 6, 26 May 1989, Pages 479–483]. *Chem. Phys. Lett.* **2013**, *589*, 35. [[CrossRef](#)]
54. Karton, A. Quantum mechanical thermochemical predictions 100 years after the Schrodinger equation. *Annu. Rep. Comput. Chem.* **2022**, *18*, 123–166.
55. Dunning, T.H. Gaussian Basis Sets for Use In Correlated Molecular Calculations. I. The Atoms Boron Through Neon and Hydrogen. *J. Chem. Phys.* **1989**, *90*, 1007–1023. [[CrossRef](#)]
56. Perdew, J.P.; Burke, K.; Ernzerhof, M. Generalized Gradient Approximation Made Simple. *Phys. Rev. Lett.* **1996**, *77*, 3865–3868. [[CrossRef](#)] [[PubMed](#)]
57. Becke, A.D. Density-functional exchange-energy approximation with correct asymptotic behavior. *Phys. Rev. A* **1988**, *38*, 3098–3100. [[CrossRef](#)] [[PubMed](#)]
58. Lee, C.; Yang, W.; Parr, R.G. Development of the Colle-Salvetti Correlation-Energy Formula Into a Functional of the Electron Density. *Phys. Rev. B* **1988**, *37*, 785–789. [[CrossRef](#)] [[PubMed](#)]
59. Zhao, Y.; Truhlar, D.G. A new local density functional for main-group thermochemistry, transition metal bonding, thermochemical kinetics, and noncovalent interactions. *J. Chem. Phys.* **2006**, *125*, 194101. [[CrossRef](#)]
60. Zhao, Y.; Truhlar, D.G. The M06 suite of density functionals for main group thermochemistry, thermochemical kinetics, noncovalent interactions, excited states, and transition elements: Two new functionals and systematic testing of four M06-class functionals and 12 other functionals. *Theo. Chem. Acc.* **2008**, *120*, 215–241. [[CrossRef](#)]
61. Boese, A.D.; Handy, N.C. New exchange-correlation density functionals: The role of the kinetic-energy density. *J. Chem. Phys.* **2002**, *116*, 9559–9569. [[CrossRef](#)]
62. Staroverov, V.N.; Scuseria, G.E.; Tao, J.; Perdew, J.P. Comparative assessment of a new nonempirical density functional: Molecules and hydrogen-bonded complexes. *J. Chem. Phys.* **2003**, *119*, 12129–12137. [[CrossRef](#)]
63. Becke, A.D. Density-Functional Thermochemistry. III. The Role of Exact Exchange. *J. Chem. Phys.* **1993**, *98*, 5648–5652. [[CrossRef](#)]
64. Stephens, P.J.; Devlin, F.J.; Chabalowski, C.F.; Frisch, M. Ab Initio Calculation of Vibrational Absorption and Circular Dichroism Spectra Using Density Functional Force Fields. *J. Phys. Chem.* **1994**, *98*, 11623–11627. [[CrossRef](#)]
65. Adamo, C.; Barone, V. Toward reliable density functional methods without adjustable parameters: The PBE0 model. *J. Chem. Phys.* **1999**, *110*, 6158–6170. [[CrossRef](#)]
66. Boese, A.D.; Martin, J.M.L. Development of density functionals for thermochemical kinetics. *J. Chem. Phys.* **2004**, *121*, 3405–3416. [[CrossRef](#)]
67. Chai, J.D.; Head-Gordon, M. Long-Range Corrected Hybrid Density Functionals with Damped Atom–Atom Dispersion Corrections. *Phys. Chem. Chem. Phys.* **2008**, *10*, 6615–6620. [[CrossRef](#)]
68. Yanai, T.; Tew, D.P.; Handy, N.C. A new hybrid exchange-correlation functional using the Coulomb-attenuating method (CAM-B3LYP). *Chem. Phys. Lett.* **2004**, *393*, 51–57. [[CrossRef](#)]
69. Grimme, S. Semiempirical hybrid density functional with perturbative second-order correlation. *J. Chem. Phys.* **2006**, *124*, 034108. [[CrossRef](#)]
70. Kozuch, S.; Martin, J.M.L. DSD-PBEP86: In search of the best double-hybrid DFT with spin-component scaled MP2 and dispersion corrections. *Phys. Chem. Chem. Phys.* **2011**, *13*, 20104–20107. [[CrossRef](#)] [[PubMed](#)]
71. Grimme, S. Density functional theory with London dispersion corrections. *WIREs Comput. Mol. Sci.* **2011**, *1*, 211–228. [[CrossRef](#)]

72. Grimme, S.; Antony, J.; Ehrlich, S.; Krieg, H. A Consistent and Accurate Ab Initio Parametrization of Density Functional Dispersion Correction (DFT-D) for the 94 Elements H-Pu. *J. Chem. Phys.* **2010**, *132*, 154104. [[CrossRef](#)] [[PubMed](#)]
73. Becke, A.D.; Johnson, E.R. Exchange-Hole Dipole Moment and the Dispersion Interaction. *J. Chem. Phys.* **2005**, *122*, 154104. [[CrossRef](#)]
74. Grimme, S.; Ehrlich, S.; Goerigk, L. Effect of the Damping Function in Dispersion Corrected Density Functional Theory. *J. Comput. Chem.* **2011**, *32*, 1456–1465. [[CrossRef](#)] [[PubMed](#)]
75. Frisch, M.J.; Trucks, G.W.; Schlegel, H.B.; Scuseria, G.E.; Robb, M.A.; Cheeseman, J.R.; Scalmani, G.; Barone, V.; Petersson, G.A.; Nakatsuji, H.; et al. *Gaussian 16 Revision B.01*; Gaussian Inc.: Wallingford, CT, USA, 2016.
76. Purvis, G.D.; Bartlett, R.J. A Full Coupled-Cluster Singles and Doubles Model: The Inclusion of Disconnected Triples. *J. Chem. Phys.* **1982**, *76*, 1910–1918. [[CrossRef](#)]
77. Stanton, J.F.; Gauss, J.; Watts, J.D.; Bartlett, R.J. A Direct Product Decomposition Approach for Symmetry Exploitation in Many-Body Methods. I. Energy Calculations. *J. Chem. Phys.* **1991**, *94*, 4334–4345. [[CrossRef](#)]
78. Prascher, B.P.; Woon, D.E.; Peterson, K.A.; Dunning, T.H.; Wilson, A.K. Gaussian Basis Sets for Use in Correlated Molecular Calculations. VII. Valence, Core-valence, and Scalar Relativistic Basis sets for Li, Be, Na, and Mg. *Theor. Chem. Acc.* **2011**, *128*, 69–82. [[CrossRef](#)]
79. Peterson, K.A.; Dunning, T.H. Accurate Correlation Consistent Basis Sets for Molecular Core-Valence Correlation Effects: The Second Row Atoms Al–Ar, and the First Row Atoms B–Ne Revisited. *J. Chem. Phys.* **2002**, *117*, 10548–10560. [[CrossRef](#)]
80. Spackman, P.R.; Jayatilaka, D.; Karton, A. Basis Set Convergence of CCSD(T) Equilibrium Geometries Using a Large and Diverse Set of Molecular Structures. *J. Chem. Phys.* **2016**, *145*, 104101. [[CrossRef](#)]
81. Gauss, J.; Stanton, J.F. Analytic CCSD(T) Second Derivatives. *Chem. Phys. Lett.* **1997**, *276*, 70–77. [[CrossRef](#)]
82. Stanton, J.F.; Gauss, J.; Cheng, L.; Harding, M.E.; Matthews, D.A.; Szalay, P.G. CFOUR, Coupled-Cluster Techniques for Computational Chemistry, a Quantum-Chemical Program Package. With Contributions from A.A. Auer, R.J. Bartlett, U. Benedikt, C. Berger, D.E. Bernholdt, Y.J. Bomble, O. Christiansen, F. Engel, R. Faber, M. Heckert, O. Heun, M. Hilgenberg, C. Huber, T.-C. Jagau, D. Jonsson, J. Jusélius, T. Kirsch, K. Klein, W.J. Lauderdale, F. Lipparini, T. Metzroth, L.A. Mück, D.P. O'Neill, D.R. Price, E. Prochnow, C. Puzzarini, K. Ruud, F. Schiffmann, W. Schwalbach, C. Simmons, S. Stopkowitz, A. Tajti, J. Vázquez, F. Wang, J.D. Watts and the Integral Packages MOLECULE (J. Almlöf and P.R. Taylor), PROPS (P.R. Taylor), ABACUS (T. Helgaker, H.J. Aa. Jensen, P. Jørgensen, and J. Olsen), and ECP Routines by A. V. Mitin and C. van Wüllen. Available online: <http://www.cfour.de> (accessed on 15 July 2023).
83. Perdew, J.P.; Schmidt, K. Jacob's ladder of density functional approximations for the exchange-correlation energy. *AIP Conf. Proc.* **2000**, *577*, 1.
84. Ceselin, G.; Salta, Z.; Bloino, J.; Tasinato, N.; Barone, V. Accurate Quantum Chemical Spectroscopic Characterization of Glycolic Acid: A Route Toward its Astrophysical Detection. *J. Phys. Chem. A* **2022**, *126*, 2373–2387. [[CrossRef](#)]
85. Ceselin, G.; Barone, V.; Tasinato, N. Accurate Biomolecular Structures by the Nano-LEGO Approach: Pick the Bricks and Build Your Geometry. *J. Chem. Theory Comput.* **2021**, *17*, 7290–7311. [[CrossRef](#)] [[PubMed](#)]
86. Barone, V.; Ceselin, G.; Fuse, M.; Tasinato, N. Accuracy Meets Interpretability for Computational Spectroscopy by Means of Hybrid and Double-Hybrid Functionals. *Front. Chem.* **2020**, *8*, 584203. [[CrossRef](#)]
87. Bousseffi, R.; Ceselin, G.; Tasinato, N.; Barone, V. DFT meets the segmented polarization consistent basis sets: Performances in the computation of molecular structures, rotational and vibrational spectroscopic properties. *J. Mol. Struct.* **2020**, *1208*, 127886. [[CrossRef](#)]
88. Karton, A.; Spackman, P.R. Evaluation of Density Functional Theory for A Large and Diverse Set of Organic and Inorganic Equilibrium Structures. *J. Comput. Chem.* **2021**, *42*, 1590–1601.
89. Martin, J.; Santra, G. Empirical Double-Hybrid Density Functional Theory: A 'Third Way' In Between WFT and DFT. *Isr. J. Chem.* **2020**, *60*, 787–804. [[CrossRef](#)]
90. DePinto, J.T.; McMahon, R.J. Structure and rearrangements of 1,3-diphenylpropynylidene. *J. Am. Chem. Soc.* **1993**, *115*, 12573–12574. [[CrossRef](#)]
91. DePinto, J.T.; deProphetis, W.A.; Menke, J.L.; McMahon, R.J. Triplet 1,3-Diphenylpropynylidene (Ph-C-C-C-Ph). *J. Am. Chem. Soc.* **2007**, *129*, 2308–2315. [[CrossRef](#)] [[PubMed](#)]
92. Sateesh, B.; Srinivas Reddy, A.; Narahari Sastry, G. Towards Design of the Smallest Planar Tetracoordinate Carbon and Boron Systems. *J. Comput. Chem.* **2007**, *28*, 335–343. [[CrossRef](#)] [[PubMed](#)]
93. Priyakumar, U.; Reddy, A.; Sastry, G. The Design of Molecules Containing Planar Tetracoordinate Carbon. *Tetrahedron Lett.* **2004**, *45*, 2495–2498. [[CrossRef](#)]

Disclaimer/Publisher's Note: The statements, opinions and data contained in all publications are solely those of the individual author(s) and contributor(s) and not of MDPI and/or the editor(s). MDPI and/or the editor(s) disclaim responsibility for any injury to people or property resulting from any ideas, methods, instructions or products referred to in the content.